This paper was published in Optics Express and is made available as an electronic reprint with the permission of OSA. The paper can be found at the following URL on the OSA website:http://www.opticsinfobase.org/abstract.cfm?URI=oe-18-2-1430. Systematic or multiple reproduction or distribution to multiple locations via electronic or other means is prohibited and is subject to penalties under law.

High-order temporal coherences of chaotic and laser light

Martin J. Stevens[1,*], Burm Baek[1], Eric A. Dauler[2,3], Andrew J. Kerman[3], Richard J. Molnar[3], Scott A. Hamilton[3], Karl K. Berggren[2], Richard P. Mirin[1] and Sae Woo Nam[1]

[1] *National Institute of Standards and Technology, 325 Broadway, Boulder, CO 80305 U.S.A.*
[2] *Research Laboratory of Electronics, Massachusetts Institute of Technology, Cambridge, Massachusetts 02139, U.S.A.*
[3] *Lincoln Laboratory, Massachusetts Institute of Technology, Lexington, Massachusetts 02420, U.S.A.*
**marty@nist.gov*

Abstract: We demonstrate a new approach to measuring high-order temporal coherences that uses a four-element superconducting nanowire single-photon detector. The four independent, interleaved single-photon-sensitive elements parse a single spatial mode of an optical beam over dimensions smaller than the minimum diffraction-limited spot size. Integrating this device with four-channel time-tagging electronics to generate multi-start, multi-stop histograms enables measurement of temporal coherences up to fourth order for a continuous range of all associated time delays. We observe high-order photon bunching from a chaotic, pseudo-thermal light source, measuring maximum third- and fourth-order coherence values of 5.87 ± 0.17 and 23.1 ± 1.8, respectively, in agreement with the theoretically predicted values of 3! = 6 and 4! = 24. Laser light, by contrast, is confirmed to have coherence values of approximately 1 for second, third and fourth orders at all time delays.

2010 Optical Society of America

OCIS codes: (270.1670) Coherent optical effects; (270.5290) Photon statistics; (040.5570) Quantum detectors; (030.5260) Photon counting.

References and links

1. R. Rigler, and E. Elson, eds., *Fluorescence Correlation Spectroscopy: Theory and Applications* (Springer-Verlag, Berlin, 2001).
2. R. Pecora, ed., *Dynamic Light Scattering: Applications of Photon Correlation Spectroscopy* (Plenum Press, New York, 1985).
3. H. J. Kimble, M. Dagenais, and L. Mandel, "Photon Antibunching in Resonance Fluorescence," Phys. Rev. Lett. **39**(11), 691–695 (1977).
4. R. Loudon, *The Quantum Theory of Light*, Third Edition (Oxford University Press, Oxford, 2000).
5. H. Qian, and E. L. Elson, "Fluorescence correlation spectroscopy with high-order and dual-color correlation to probe nonequilibrium steady states," Proc. Natl. Acad. Sci. U.S.A. **101**(9), 2828–2833 (2004).
6. P.-A. Lemieux, and D. J. Durian, "Investigating non-Gaussian scattering processes by using *n*th-order intensity correlation functions," J. Opt. Soc. Am. A **16**(7), 1651–1664 (1999).
7. E. A. Burt, R. W. Ghrist, C. J. Myatt, M. J. Holland, E. A. Cornell, and C. E. Wieman, "Coherence, Correlations, and Collisions: What One Learns about Bose-Einstein Condensates from Their Decay," Phys. Rev. Lett. **79**(3), 337–340 (1997).
8. H. Deng, G. Weihs, C. Santori, J. Bloch, and Y. Yamamoto, "Condensation of semiconductor microcavity exciton polaritons," Science **298**(5591), 199–202 (2002).
9. J. Wiersig, C. Gies, F. Jahnke, M. Aßmann, T. Berstermann, M. Bayer, C. Kistner, S. Reitzenstein, C. Schneider, S. Höfling, A. Forchel, C. Kruse, J. Kalden, and D. Hommel, "Direct observation of correlations between individual photon emission events of a microcavity laser," Nature **460**(7252), 245–249 (2009).
10. M. Assmann, F. Veit, M. Bayer, M. van der Poel, and J. M. Hvam, "Higher-order photon bunching in a semiconductor microcavity," Science **325**(5938), 297–300 (2009).
11. A. G. Palmer 3rd, and N. L. Thompson, "Molecular aggregation characterized by high order autocorrelation in fluorescence correlation spectroscopy," Biophys. J. **52**(2), 257–270 (1987).
12. R. Hanbury Brown, and R. Q. Twiss, "Correlations between photons in two coherent beams of light," Nature **177**(4497), 27–29 (1956).

#119517 - $15.00 USD   Received 18 Nov 2009; revised 23 Dec 2009; accepted 26 Dec 2009; published 12 Jan 2010

13. R. F. Chang, V. Korenman, C. O. Alley, and R. W. Detenbeck, “Correlations in Light from a Laser at Threshold,” Phys. Rev. **178**(2), 612–621 (1969).
14. M. Corti, and V. Degiorgio, “Intrinsic third-order correlations in laser light near threshold,” Phys. Rev. A **14**(4), 1475–1478 (1976).
15. Y. Qu, S. Singh, and C. D. Cantrell, “Measurements of higher order photon bunching of light beams,” Phys. Rev. Lett. **76**(8), 1236–1239 (1996).
16. G. N. Gol’tsman, O. Okunev, G. Chulkova, A. Lipatov, A. Semenov, K. Smirnov, B. Voronov, A. Dzardanov, C. Williams, and R. Sobolewski, “Picosecond superconducting single-photon optical detector,” Appl. Phys. Lett. **79**(6), 705 (2001).
17. K. M. Rosfjord, J. K. W. Yang, E. A. Dauler, A. J. Kerman, V. Anant, B. M. Voronov, G. N. Gol’tsman, and K. K. Berggren, “Nanowire single-photon detector with an integrated optical cavity and anti-reflection coating,” Opt. Express **14**(2), 527–534 (2006).
18. E. A. Dauler, A. J. Kerman, B. S. Robinson, J. K. W. Yang, B. Voronov, G. Goltsman, S. A. Hamilton, and K. K. Berggren, “Photon-number-resolution with sub-30-ps timing using multi-element superconducting nanowire single photon detectors,” J. Mod. Opt. **56**(2), 364–373 (2009).
19. F. Davidson, “Measurements of Photon Correlations in a Laser Beam near Threshold with Time-to-Amplitude Converter Techniques,” Phys. Rev. **185**(2), 446–453 (1969).
20. A. Verevkin, A. Pearlman, W. Słysz, J. Zhang, M. Currie, A. Korneev, G. Chulkova, O. Okunev, P. Kouminov, K. Smirnov, B. Voronov, G. N. Gol’tsman, and R. Sobolewski, “Ultrafast superconducting single-photon detectors for near-infrared-wavelength quantum communications,” J. Mod. Opt. **51**, 1447 (2004).
21. A. J. Kerman, E. A. Dauler, W. E. Keicher, J. K. W. Yang, K. K. Berggren, G. Gol’tsman, and B. Voronov, “Kinetic-inductance- limited reset time of superconducting nanowire photon counters,” Appl. Phys. Lett. **88**(11), 111116 (2006).
22. R. H. Hadfield, M. J. Stevens, S. S. Gruber, A. J. Miller, R. E. Schwall, R. P. Mirin, and S. W. Nam, “Single photon source characterization with a superconducting single photon detector,” Opt. Express **13**(26), 10846–10853 (2005).
23. E. A. Dauler, M. J. Stevens, B. Baek, R. J. Molnar, S. A. Hamilton, R. P. Mirin, S. W. Nam, and K. K. Berggren, “Measuring intensity correlations with a two-element superconducting nanowire single-photon detector,” Phys. Rev. A **78**(5), 053826 (2008).
24. R. J. Glauber, “Optical Coherence and Photon Statistics,” in *Quantum Optics and Electronics (Les Houches 1964)*, C. deWitt, A. Blandin and C. Cohen-Tannoudji, eds. (Gordon and Breach, New York, 1965). pp. 63–185.
25. F. Boitier, A. Godard, E. Rosencher, and C. Fabre, “Measuring photon bunching at ultrashort timescale by two-photon absorption in semiconductors,” Nat. Phys. **5**(4), 267–270 (2009).
26. A. Ofir, and E. N. Ribak, “Offline, multidetector intensity interferometers – I. Theory,” Mon. Not. R. Astron. Soc. **368**(4), 1646–1651 (2006).
27. I. N. Agafonov, M. V. Chekhova, T. Sh. Iskhakov, and L.-A. Wu, “High-visibility intensity interference and ghost imaging with pseudo-thermal light,” J. Mod. Opt. **56**(2), 422–431 (2009).
28. J. Liu, and Y. Shih, “Nth-order coherence of thermal light,” Phys. Rev. A **79**(2), 023819 (2009).

---

1. Introduction

The temporal coherence of an optical field contains information about dynamic processes in a light source and in any subsequent media with which the light interacts. Photon-correlation techniques that measure temporal coherences have furthered our understanding of a wide variety of physical systems. For example, the dynamics of chemical reactions on a few-molecule scale can be accessed via Fluorescence Correlation Spectroscopy [1] or Dynamic Light Scattering [2]. In quantum optics, the quality of a single-photon source—an essential component in many quantum information protocols—is gauged by how close the second-order coherence is to the ideal value of zero [3]. Coherences higher than second order are not routinely measured, even though they can reveal new information, in part because of the added experimental complexity.

The second-, third- and fourth-order temporal coherences can be defined in terms of the creation ($\hat{a}^\dagger$) and annihilation ($\hat{a}$) operators as [4]

$$g^{(2)}(\tau) = \frac{\left\langle \hat{a}^\dagger(t)\hat{a}^\dagger(t+\tau)\hat{a}(t+\tau)\hat{a}(t)\right\rangle}{\left\langle \hat{a}^\dagger(t)\hat{a}(t)\right\rangle^2}, \tag{1}$$

#119517 - $15.00 USD Received 18 Nov 2009; revised 23 Dec 2009; accepted 26 Dec 2009; published 12 Jan 2010

$$g^{(3)}(\tau_1,\tau_2)=\frac{\left\langle \hat{a}^\dagger(t)\hat{a}^\dagger(t+\tau_1)\hat{a}^\dagger(t+\tau_2)\hat{a}(t+\tau_2)\hat{a}(t+\tau_1)\hat{a}(t)\right\rangle}{\left\langle \hat{a}^\dagger(t)\hat{a}(t)\right\rangle^3}, \qquad (2)$$

$$g^{(4)}(\tau_1,\tau_2,\tau_3)=\frac{\left\langle \hat{a}^\dagger(t)\hat{a}^\dagger(t+\tau_1)\hat{a}^\dagger(t+\tau_2)\hat{a}^\dagger(t+\tau_3)\hat{a}(t+\tau_3)\hat{a}(t+\tau_2)\hat{a}(t+\tau_1)\hat{a}(t)\right\rangle}{\left\langle \hat{a}^\dagger(t)\hat{a}(t)\right\rangle^4}, \quad (3)$$

where < > indicates an average over time, t, and the τ's are time delays. Loss does not change the coherence properties of a light field, provided all modes experience the same loss [4]; as a result, coherences can be measured accurately even with low detection efficiencies. Because $g^{(2)}(\tau)$ has the form of an autocorrelation, it must be symmetric about τ. Asymmetry in $g^{(3)}(\tau_1,\tau_2)$, which lacks this constraint, can indicate irreversible processes, which can be used to distinguish a non-equilibrium steady-state from true equilibrium in chemical reactions, for example [5]. In Dynamic Light Scattering experiments, the scattering processes are generally presumed to obey Gaussian statistics, in which case higher-order coherences can be accurately predicted from measured second-order coherences using generalized Siegert relations; measured higher-order coherences that violate these relations can indicate the presence of non-Gaussian scattering processes [6]. Third- and fourth-order coherences have also been predicted or demonstrated to contain new information about atomic [7] and polaritonic [8] condensates, microcavity lasers [9,10] and molecular aggregates [11].

Often, $g^{(2)}(\tau)$ is measured with a Hanbury Brown-Twiss interferometer [12] consisting of a beamsplitter, two discrete single-photon detectors, and timing electronics that record the number of instances in which photons registered by the two detectors are delayed by τ. Ideally, the beamsplitter projects one incoming optical mode onto two identical output modes, so that both detectors sample light from the same spatial mode. In principle, this technique can be scaled to measure higher-order coherences by adding more beamsplitters and detectors, provided that the timing electronics have a sufficient number of independent channels. However, the increased experimental complexity can introduce unwanted artifacts if there is optical or electrical crosstalk between any of the detectors, or if the detectors do not all sample the same spatial mode(s), either because of imperfect beamsplitters or misalignment. Nearly all previous measurements [6,11,13–15] of $g^{(3)}(\tau_1,\tau_2)$ and $g^{(4)}(\tau_1,\tau_2,\tau_3)$ were performed with only one or two detectors, and zero-delay values could only be extrapolated from measured data at non-zero delays, due to finite detector and electronics dead times [11].

Here, we demonstrate a more direct approach to measuring higher-order coherences that uses a four-element superconducting nanowire single-photon detector (SNSPD) [16,17] in which four independent, single-photon-sensitive elements are interleaved over a single spatial mode of the optical beam [18]. We show the power of this technique by measuring n^{th}-order coherences (n = 2,3,4) both of a chaotic, pseudo-thermal source that exhibits strong photon bunching consistent with the expected $g^{(n)}(0,0,...,0) = n!$, and of laser light, for which $g^{(n)}(\tau_1,\tau_2,...,\tau_{n-1}) \approx 1$. Whereas previous measurements of $g^{(3)}(\tau_1,\tau_2)$ and $g^{(4)}(\tau_1,\tau_2,\tau_3)$ were limited to investigating correlations where at least one of the time delays was fixed [6,9–11,13–15,19], here we measure them for continuous ranges of all delays, offering more complete insight into the nature of high-order photon bunching. These results demonstrate that using multiple detector elements to parse an optical beam over dimensions smaller than the minimum diffraction-limited spot size can be equivalent—and in some cases superior—to using beamsplitters and discrete detectors that each sample a replica of the entire mode.

2. Experiment

The four-element SNSPD is shown in Fig. 1. Each element is an independent single-photon detector, consisting of a current-biased superconducting nanowire that is driven into a resistive state—thus delivering an output voltage pulse—upon absorption of one photon [16].

#119517 - $15.00 USD Received 18 Nov 2009; revised 23 Dec 2009; accepted 26 Dec 2009; published 12 Jan 2010

SNSPDs combine high speed with spectral sensitivity spanning from ultraviolet to near-infrared [20]. Devices with sub-30 ps timing jitter [18,20], dead time < 5 ns [21], and detection efficiency exceeding 50% [17] have recently been demonstrated. Light is coupled to the device, which is held at a temperature of ~3 K in a closed-cycle helium cryocooler, through a single-mode optical fiber [22]. The active area of the four-element SNSPD is matched to the mode field diameter of this fiber, allowing all four interleaved nanowire elements to equally sample a single spatial mode. Each element of the SNSPD—which has not been optimized with optical coatings [17]—has a system detection efficiency of ~1% at 1550 nm and a dark count rate of ~100 Hz. Each element is independently biased and read out, leading to little or no spurious cross-correlation between the elements.

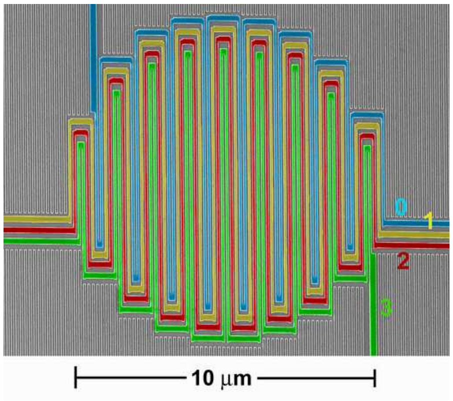

Fig. 1. Scanning-electron microscope image of the four-element SNSPD, with nanowire elements 0-3 traced out in color. Each element consists of a ~5 nm-thick × 80 nm-wide NbN nanowire on a sapphire substrate, with 60 nm gaps between wires. The 9.4 μm-diameter active area is well matched to the spatial mode of a single mode optical fiber, the cleaved end of which is held within ~10 μm of the detector surface. The interleaved design ensures that all four elements equally sample this spatial mode.

Fast, four-channel electronics record photon arrival times on each element. These time-tag data are post-processed to obtain multi-start, multi-stop correlation histograms between two, three and four SNSPD elements. To compute $g^{(2)}(\tau)$, $g^{(3)}(\tau_1,\tau_2)$ and $g^{(4)}(\tau_1,\tau_2,\tau_3)$, the raw histograms are normalized by the number of counts expected in each bin for uncorrelated events, $r_0r_1\Delta\tau T$, $r_0r_1r_2(\Delta\tau)^2T$ and $r_0r_1r_2r_3(\Delta\tau)^3T$, respectively, where r_i is the measured count rate on element i, $\Delta\tau = 60$ ns is the histogram bin width, T is the integration time, and τ_i is the delay between a photon registered by element 0 and a photon registered by element $i = 1, 2, 3$. To reduce errors due to slow variations in count rates, the data are piece-wise normalized, 4×10^6 time stamps (4 to 10 s) at a time. The $g^{(2)}(\tau)$ data are averages of the six measured two-channel correlation histograms: 0-1, 0-2, 0-3, 1-2, 1-3 and 2-3. Likewise, the $g^{(3)}(\tau_1,\tau_2)$ data are averages of four three-channel histograms: 0-1-2, 0-1-3, 0-2-3 and 1-2-3.

The combined timing jitter of the SNSPD and electronics is ~50 ps, permitting the investigation of processes with much shorter coherence times than most prior work. Furthermore, having four independent detector elements and timing channels with no inter-element or inter-channel dead time and virtually no crosstalk allows us to measure temporal coherences for arbitrary values of all delays, including the origin, $\tau_1 = \tau_2 = \tau_3 = 0$, which is often the most relevant point. Recently, we demonstrated that two adjacent (non-interleaved) SNSPD elements can be used to accurately measure the second-order coherence [23].

We measure coherences for two sources. One source is a single-mode, 1070 nm-wavelength diode laser, operated well above threshold and attenuated with neutral density filters, coupled into a single-mode optical fiber and directed to the four-element SNSPD. The laser should exhibit all the properties of a coherent source, with $g^{(n)}(\vec{\tau}) = 1$ for all n and all

#119517 - $15.00 USD Received 18 Nov 2009; revised 23 Dec 2009; accepted 26 Dec 2009; published 12 Jan 2010
(C) 2010 OSA

$\vec{\tau} = \left(\tau_1, \tau_2 \ldots \tau_{n-1}\right)$ [4,24]. The other source is a chaotic, pseudo-thermal source, in which the attenuated laser light is scattered off of a rotating ground glass disk, and the resulting speckle pattern is sampled in the far field with the fiber and again directed to the four-element SNSPD. This source should exhibit bunching: for an ideal, single-mode chaotic source, $g^{(n)}\left(\vec{0}\right) = n!$ at the origin, where all delays are zero, and $g^{(n)} \to 1$ for $\tau_i >> \tau_c$ for all i and $(\tau_i - \tau_j) >> \tau_c$ for all $i \neq j$, where τ_c is the source coherence time [4,6]. For both sources, a polarizer before the fiber launch and microbends in the fiber (which is designed for a wavelength of 1550 nm) ensure that the light reaching the detector is single mode.

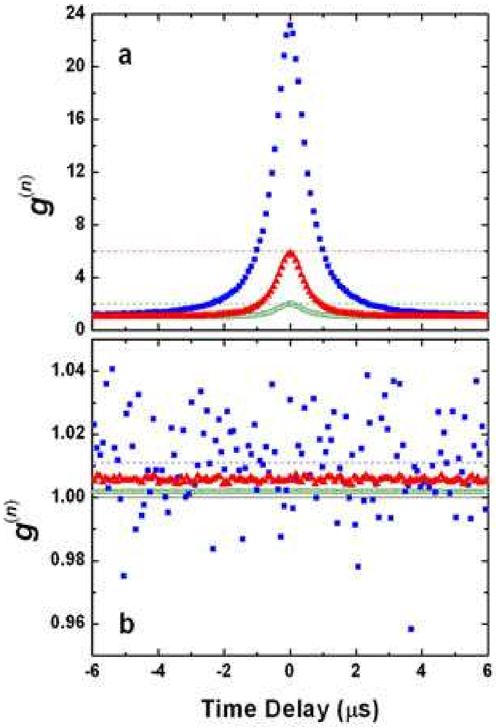

Fig. 2. Measured n^{th}-order temporal coherences for $n = 2$ (○), 3 (▲) and 4 (■). (a) Chaotic source data. The magnitude of photon bunching scales roughly as $n!$, as can be seen from the expected peak $g^{(2)}$, $g^{(3)}$ and $g^{(4)}$ values of 2 (dashed green line), 6 (dashed red line) and 24 (top axis). (b) Laser source data, also showing the expected value of 1 (black line) and the mean measured $g^{(4)}$ value of 1.011 (dashed blue line). In both (a) and (b), the $g^{(2)}$ data are displayed as a function of τ, while the $g^{(3)}$ and $g^{(4)}$ data are plotted against parameterized delays that measure temporal distance from the origin, $\tau_{P3} = \pm(\tau_1^2 + \tau_2^2)^{1/2}$ and $\tau_{P4} = \pm(\tau_1^2 + \tau_2^2 + \tau_3^2)^{1/2}$, respectively, where ± is determined by the sign of τ_1. These trace out cross sections from $(\tau_1, \tau_2) = (-6/\sqrt{2}\ \mu s, 6/\sqrt{2}\ \mu s)$ to $(6/\sqrt{2}\ \mu s, -6/\sqrt{2}\ \mu s)$ and (τ_1, τ_2, τ_3) from (-4 μs, 2 μs, 4 μs) to (4 μs, -2 μs, -4 μs).

3. Results and discussion

Measured coherences are shown in Fig. 2. The chaotic source data are bunched around the origin and decrease to ~1 as the delays increase beyond ~ ± 4 μs. The second-order coherence reaches a peak value of $g^{(2)}(0) = 1.985 \pm 0.019$ for the 60 ns-wide bin centered at the origin, less than one standard deviation away from the expected value of 2. The peak $g^{(3)}$ and $g^{(4)}$ values of 5.87 ± 0.17 and 23.1 ± 1.8 are in agreement with the values of $3! = 6$ and $4! = 24$ expected for a chaotic source. A very different result is observed from the laser source. All these data lie close to the expected value of 1 for all delays, indicating that this source is highly coherent at least to fourth order. Averaging these coherent source data over delays

#119517 - $15.00 USD Received 18 Nov 2009; revised 23 Dec 2009; accepted 26 Dec 2009; published 12 Jan 2010
(C) 2010 OSA

ranging from $-6\ \mu$s to $+\ 6\ \mu$s yields mean values of 1.0018 ± 0.0008 for $g^{(2)}$, 1.006 ± 0.002 for $g^{(3)}$, and 1.011 ± 0.005 for $g^{(4)}$.

Third-order coherence data for the chaotic source are shown in Fig. 3(a) for a more complete set of delays τ_1 and τ_2. The strongest bunching occurs around the origin, where each of the three elements registers a photon simultaneously and $g^{(3)}(0,0) = 5.87$. This result indicates that the probability of three elements firing at the same time is nearly 6 times higher than the probability of the elements firing at three (particular) different times. The three ridges, which intersect the origin along lines at $\tau_1 = 0$, $\tau_2 = 0$ and $\tau_1 = \tau_2$, correspond to two of the three elements firing simultaneously; $g^{(3)}$ reaches a peak value of ~2 along each of these ridges. Far from the origin and away from the ridges, $g^{(3)} \approx 1$, as expected for uncorrelated events.

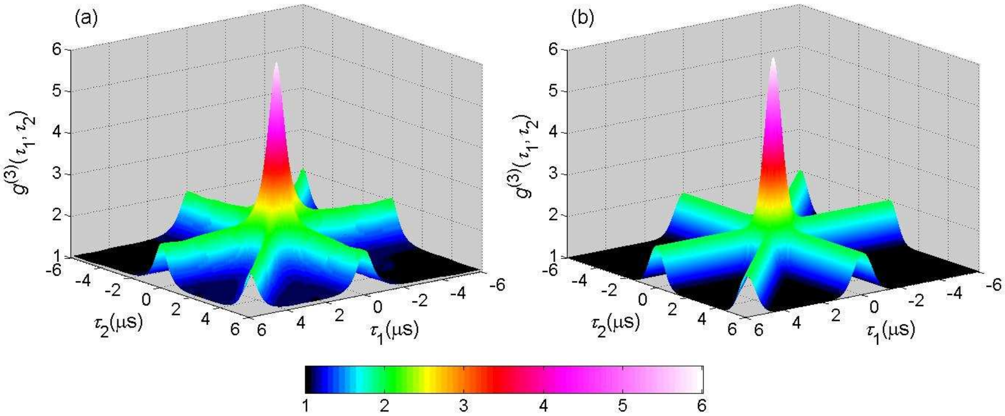

Fig. 3. (a) Measured third-order coherence from the chaotic source, where both color and height indicate measured value of $g^{(3)}$. The cross-section in Fig. 2(a) samples these data along a diagonal line (not shown) extending from the far left corner to the far right corner as plotted here. (b) Calculated third-order coherence for a chaotic source derived from an ideal Gaussian scattering process with a coherence time of 900 ns, as discussed in the text.

The fourth-order coherence data from the chaotic source are shown in the left column of Fig. 4 and Media 1, where each frame represents a slice of the data for a fixed value of τ_3. For $\tau_3 = 0$, when elements 0 and 3 detect photons simultaneously, the data appear qualitatively similar to the $g^{(3)}$ data in Fig. 3(a), but the values are significantly higher: $g^{(4)}$ reaches its peak value of 23.1 at the origin, where all four elements fire at the same time, and decreases to ~2.1 far from the origin. Slices at nonzero values of τ_3 have even richer structure. In the black regions, the four elements detect photons at four different times, and $g^{(4)}$ is close to the value of 1 expected for uncorrelated events. At the center of the dark blue bands, where just two of the four elements register a photon at once, $g^{(4)}$ reaches a value of ~2. In the small light blue areas where any two of these bands cross, the value increases to ~4, corresponding to two elements firing at one time and the other two elements firing at a different time. Events where

#119517 - $15.00 USD   Received 18 Nov 2009; revised 23 Dec 2009; accepted 26 Dec 2009; published 12 Jan 2010
(C) 2010 OSA

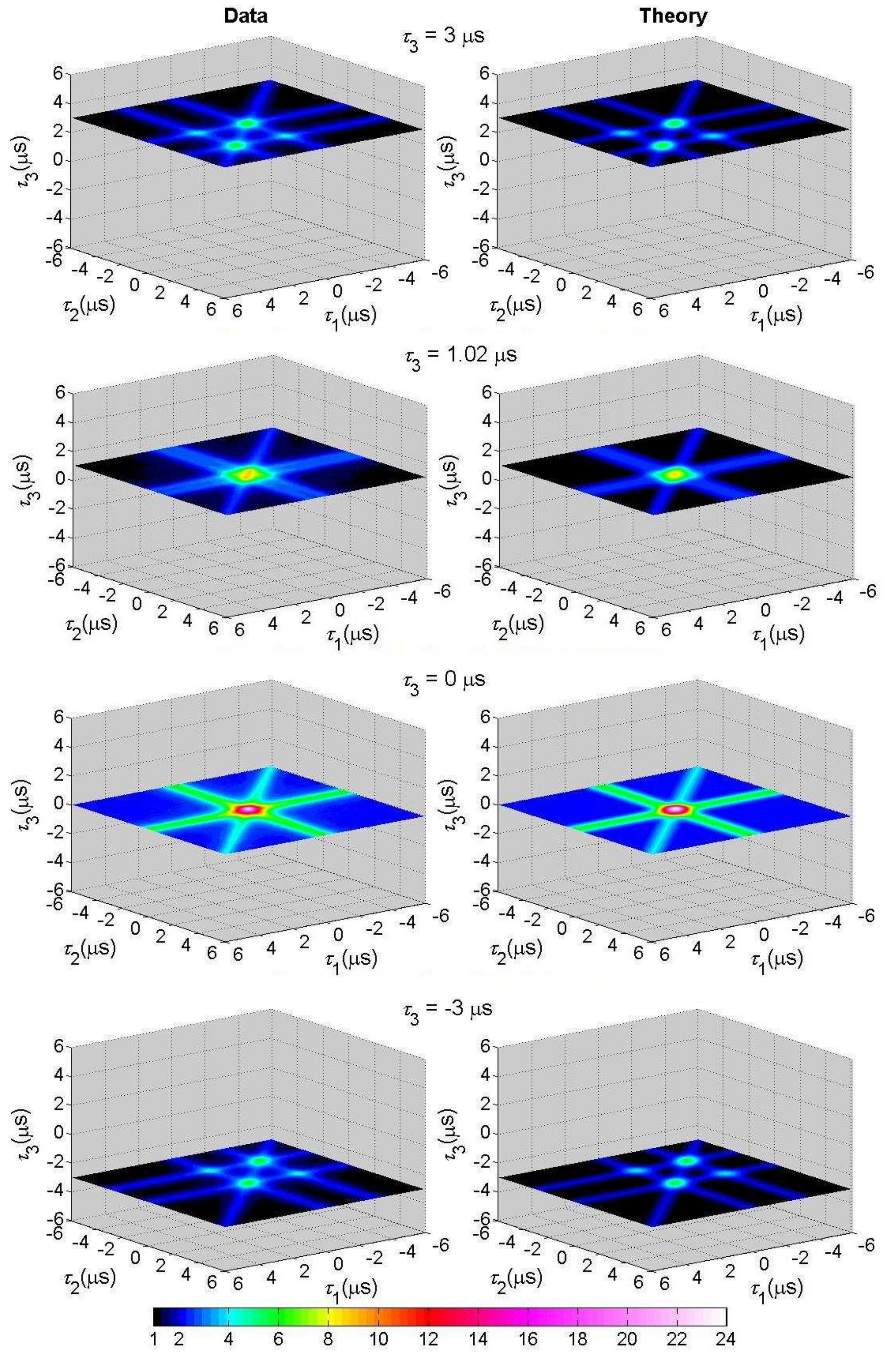

Fig. 4. Four frames from a movie (Media 1) of fourth-order coherence data (left) and theory (right) for the chaotic source for four values of τ_3. Color bar at the bottom shows $g^{(4)}$ values.

three elements register photons simultaneously appear as larger green areas where three bands intersect and $g^{(4)} \approx 6$.

The primary source of experimental uncertainty is a slow variation in the measured coherences. For the chaotic source, this variation is likely due to time-dependent leakage of an additional mode [6] to the multi-element detector. For the coherent source, the more likely culprit is a time-dependence to the weak cross-correlation between channels evidenced by the small, yet statistically significant, deviation from 1 of $g^{(n)}$. This cross-correlation has a 60 Hz component, suggestive of laser intensity fluctuations or pickup in the external biasing and/or readout electronics. For delays <5 ns, we observe somewhat larger variations (not shown), with $g^{(2)}(\tau)$ ranging between ~0.98 and ~1.02. This variation could indicate crosstalk in the external electronics or among the elements themselves; nonetheless, the impact is minimal for the 60 ns histogram bin widths used here.

Although the coherences in Eqs. (1)-(3) are defined in terms of the quantized field operators $\hat{a}$ and $\hat{a}^\dagger$, a chaotic source can be modeled by calculating intensity correlations for a classical field with chaotic fluctuations [4]. We have computed the quantities

$$g^{(3)}(\tau_1,\tau_2) = \frac{\langle I(t) I(t+\tau_1) I(t+\tau_2)\rangle}{\langle I(t)\rangle^3}$$

$$g^{(4)}(\tau_1,\tau_2,\tau_3) = \frac{\langle I(t) I(t+\tau_1) I(t+\tau_2) I(t+\tau_3)\rangle}{\langle I(t)\rangle^4}$$

for a chaotic source assuming an ideal Gaussian scattering process with a coherence time of 900 ns, following the method of Lemieux and Durian [6]. The calculated $g^{(3)}$ [Fig. 3(b)] and $g^{(4)}$ (Fig. 4, right column) reproduce all the major features visible in the data, reaching values of $g^{(3)}(0,0) = 6$ and $g^{(4)}(0,0,0) = 24$ at the origins. The excellent agreement between data and theory for the Gaussian process studied here, for which knowledge of $g^{(2)}(\tau)$ could have been used to determine the higher-order coherences [6,24], confirms that our technique is sound. Our apparatus, which has a timing jitter of ~50 ps, could be used to characterize much faster processes than the sources studied here. While this time resolution does not rival that of a recent $g^{(2)}(\tau)$ measurement relying on detector nonlinearities [25], our technique is linear, and thus is suitable for states with low mean photon number.

We anticipate that higher-order temporal coherence measurements with multi-element SNSPDs could further our understanding of the dynamics of non-Gaussian processes such as quantum condensates [7,8], molecular aggregates [11], fractal diffusers, single-photon sources [3], and biochemical reactions in non-equilibrium steady-state [5]. Even for Gaussian processes, higher-order measurements can yield improved visibility or signal-to-noise ratio under certain conditions [26–28]. Finally, although it has long been argued [24] that $g^{(n)} = 1$ for the emission of an ideal laser, the experimental record contains limited data for coherences higher than second order. This technique could enable precision measurements of the degree of high-order coherence of laser emission.

Acknowledgments

The authors thank S. Glancy for discussions. This work made use of the Scanning Electron Beam Lithography facility in the Research Laboratory of Electronics at MIT and was sponsored in part by the United States Air Force under Air Force Contract #FA8721-05-C-0002. Opinions, interpretations, recommendations and conclusions are those of the authors and are not necessarily endorsed by the United States Government.